

Improved Convergence Rates of Anderson Acceleration for a Large Class of Fixed-Point Iterations

Casey Garner* Gilad Lerman* Teng Zhang†

November 7, 2023

Abstract

This paper studies Anderson acceleration (AA) for fixed-point methods $\mathbf{x}^{(k+1)} = q(\mathbf{x}^{(k)})$. It provides the first proof that when the operator q is linear and symmetric, AA improves the root-linear convergence factor over the fixed-point iterations. When q is nonlinear, yet has a symmetric Jacobian at the solution, a slightly modified AA algorithm is proved to have an analogous root-linear convergence factor improvement over fixed-point iterations. Simulations verify our observations. Furthermore, experiments with different data models demonstrate AA is significantly superior to the standard fixed-point methods for Tyler’s M-estimation.

Keywords: Anderson acceleration, fixed-point method, Tyler’s M-estimation

MSC codes: 65F10, 65H10, 68W40

1 Introduction

This paper investigates the convergence properties of the popular acceleration technique for fixed-point problems called Anderson acceleration (AA). The method, originally introduced by D.G. Anderson in the context of integral equations (1965), utilizes a history of prior iterates to accelerate the classical fixed-point iteration, aka the Picard iteration (Picard, 1890). A brief history of the method, including its relationship to Pulay mixing, nonlinear GMRES, and quasi-Newton methods, can be found in the literature (Fang and Saad, 2009; Kelley, 2018; Potra and Engler, 2013; Pulay, 1980). A renewed interest in AA came about following the work of Walker and Ni (2011) where they demonstrated the effectiveness of AA in numerous applications such as nonnegative matrix factorization and domain decomposition. Recently, AA has been employed in machine learning applications with some success (Geist and Scherrer, 2018; Shi et al., 2019; Sun et al., 2021).

*School of Mathematics, University of Minnesota (garne214@umn.edu, lerman@umn.edu)

†Department of Mathematics, University of Central Florida (Teng.Zhang@ucf.edu)

Despite a long history of use and strong recent interest, the accelerated convergence of AA is still not completely understood. The first mathematical convergence results for Anderson acceleration, for linear and nonlinear problems, were established by Toth and Kelley (2015); however, they only proved AA did not worsen the convergence of the fixed-point iteration. Their theory did not prove Anderson acceleration accelerated the fixed-point method as often witnessed in practice. Following Toth and Kelley, further efforts have shed more light on the convergence behavior of AA. In the papers by Evans et al. (2020), Pollock et al. (2019), and Pollock and Rebholz (2021), they proved AA improved convergence by studying the “stage- k gain” of AA which shows how much AA improves upon the fixed-point method at iteration k . Their analysis showed AA can best the fixed-point iteration by a factor $0 \leq \theta_k \leq 1$ known as the gain at step k ; however, as noted by De Sterck and He, “it is not clear how θ_k may be evaluated or bounded in practice or how it may translate to an improved linear asymptotic convergence factor” (2022). In the work of De Sterck and He (2022), the authors also note some intriguing properties of AA, such as how the linear asymptotic convergence factor depends on the initialization of the method, but they also fail to prove AA has an improved asymptotic convergence factor over the fixed-point iteration. More recently, Rebholz and Xiao (2023) prove how AA affects the convergence rate of superlinearly and sublinearly converging fixed-point iterations.

The aforementioned papers have added much to our understanding of the convergence of AA in the past decade, and this paper joins the conversation by establishing the improved root-linear convergence factor of AA over the fixed-point iteration. To the best of our knowledge, this paper is the first to present such an improvement which clearly shows AA has a better asymptotic convergence factor than the fixed-point iteration. Notably, our approach to proving the claim is novel and does not utilize the notation of gain as defined in prior works (Evans et al., 2020; Pollock et al., 2019; Pollock and Rebholz, 2021). Furthermore, our results only require common assumptions found in the literature. For example, we assume the Jacobian matrix of the operator g , for which we desire to compute fixed-points, is symmetric at fixed-points (Scieur, 2019; Scieur et al., 2016).

Before proceeding, we introduce definitions and notation; $\mathbb{R}^{n \times n}$ and $\mathcal{S}^{n \times n}$ denote the set of real n -by- n and real symmetric n -by- n matrices respectively. Given $\mathbf{A} \in \mathbb{R}^{n \times n}$, its ℓ_2 norm (or spectral/operator norm) is denoted $\|\mathbf{A}\|$ while its Frobenius norm is denoted $\|\mathbf{A}\|_F$. The largest and the smallest eigenvalues of a matrix \mathbf{A} are denoted $\lambda_{\max}(\mathbf{A})$ and $\lambda_{\min}(\mathbf{A})$ respectively. Given the vector $\mathbf{x} \in \mathbb{R}^n$, $\text{Diag}(\mathbf{x})$ denotes the diagonal matrix formed by \mathbf{x} . For any three points $O, P, Q \in \mathbb{R}^n$, $\angle OPQ \in [0, \pi]$ represents the angle between the vectors \vec{PO} and \vec{PQ} . For any sequence $\{\mathbf{x}^{(k)}\}$ that converges to \mathbf{x}_* , we define its r -linear convergence factor to be

$$\rho_{\{\mathbf{x}^{(k)}\}} = \limsup_{k \rightarrow \infty} \|\mathbf{x}_* - \mathbf{x}^{(k)}\|^{\frac{1}{k}}.$$

Then, we say $\{\mathbf{x}^{(k)}\}$ converges r -linearly with r -linear convergence factor $\rho_{\{\mathbf{x}^{(k)}\}}$, and here the prefix “ r -” stands for “root”.

The paper is organized as follows; Section 2 introduces the problem setting and defines the Anderson acceleration algorithm; Section 3 states the main results of the paper with the key result being a proven upper bound on the root-linear convergence factor for AA when the Jacobian matrix is symmetric; Section 3 while Section 4 presents numerical experiments for both linear and nonlinear operators. The paper concludes in Section 6 with directions for future inquiry. All proofs and additional experiments are provided in the supplementary materials.

2 Anderson Acceleration

This paper concerns the convergence of acceleration methods for fixed-point (FP) iterations of the type

$$\mathbf{x} = q(\mathbf{x}),$$

where $q : \mathbb{R}^n \rightarrow \mathbb{R}^n$. For this problem, the standard fixed-point iteration/method is the iterative procedure described by

$$\mathbf{x}^{(k+1)} = q(\mathbf{x}^{(k)}). \tag{1}$$

In this work, we study the Anderson acceleration algorithm with depth m , AA(m), applied to the fixed-point iteration (1). The specific version of AA(m) we study is given in Algorithm 1. The key idea behind the method is to use a history of at most $m + 1$ points to construct the next update at each iteration. A linear least-squares problem, (2), is solved at each iteration to determine how to utilize the prior iterates to form the next update. It is worth noting that any vector norm can be utilized in (2) without changing the convergence theory for Anderson acceleration. As discussed in Section 1, AA has proven very effective in many applications and this practical utility has motivated the resurgence of convergence analysis for the method.

3 Main Results

This section presents our main results showcasing Anderson acceleration has an improved r-linear convergence factor over the fixed-point iteration. Section 3.1 shows in the case of linear and symmetric operators AA(m) converges faster than the fixed-point iteration with the convergence rate given in Theorem 1. It also clarifies some very basic geometric ideas of the proof, though the intricate geometric estimates are left to the supplementary materials. Another idea that makes the proofs more elegant is a reformulation of the AA method and Section 3.2 describes it. Section 3.3 shows when q is nonlinear, yet has a symmetric Jacobian at the solution, a modified AA algorithm has an analogous root-linear convergence factor improvement over the fixed-point iteration when

Algorithm 1 Anderson acceleration algorithm AA(m)

Input: operator $q : \mathbb{R}^n \rightarrow \mathbb{R}^n$, initialization $\mathbf{x}^{(0)}$, depth m **Output:** An estimation of the fixed-point of q .

Steps:

1: $\mathbf{x}^{(1)} = q(\mathbf{x}^{(0)})$.

2: For $k \geq 2$, let $m_k = \min(m, k)$. Solve the minimization problem

$$\min_{\sum_{j=k-m_k}^k \alpha_j^{(k)} = 1} \left\| \sum_{j=k-m_k}^k \alpha_j^{(k)} (q(\mathbf{x}^{(j)}) - \mathbf{x}^{(j)}) \right\|, \quad (2)$$

and let

$$\mathbf{x}^{(k+1)} = \sum_{j=k-m_k}^k \alpha_j^{(k)} q(\mathbf{x}^{(j)}).$$

3: Repeat step 2 for $k \geq 2$ and $\lim_{\text{iter} \rightarrow \infty} \mathbf{x}^{(\text{iter})}$ is an estimation of the fixed-point.

initialized near a solution. Section 3.4 closes with additional remarks and discussion concerning our results.

3.1 Linear Operator

We begin with the convergence rate of AA for linear symmetric operators q , where $q(\mathbf{x}) = \mathbf{W}\mathbf{x} + \mathbf{a}$ with $\mathbf{W} \in \mathcal{S}^{n \times n}$ and $-1 < \lambda_{\min}(\mathbf{W}) \leq \lambda_{\max}(\mathbf{W}) < 1$. Theorem 1 establishes the convergence rate of AA(m) over every two iterations based on $\lambda_{\min}(\mathbf{W})$ and $\lambda_{\max}(\mathbf{W})$ to provide an upper bound on the r -linear convergence factor of AA(m).

Theorem 1 (Convergence factor of AA(m) for linear symmetric operators). *Let $q(\mathbf{x}) = \mathbf{W}\mathbf{x} + \mathbf{a}$ with $\mathbf{W} \in \mathcal{S}^{n \times n}$ and $\|\mathbf{W}\| < 1$. Then AA(m) converges r -linearly to a fixed-point of q with rate bounded by $\sqrt{w_0 \|\mathbf{W}\|}$ for any initialization, where*

$$w_0 = \sup_{a \geq 0} \sin \left[\sin^{-1} \left(\frac{|\lambda_{\max}(\mathbf{W}) - \lambda_{\min}(\mathbf{W})| a}{\sqrt{4 + (2 - \lambda_{\max}(\mathbf{W}) - \lambda_{\min}(\mathbf{W}))^2 a^2}} \right) + \left| \tan^{-1}(a) - \tan^{-1} \left(\left(1 - \frac{\lambda_{\max}(\mathbf{W}) + \lambda_{\min}(\mathbf{W})}{2} \right) a \right) \right| \right]. \quad (3)$$

More specifically, if $\{\mathbf{x}^{(k)}\}$ is the sequence generated by AA(m), then for all $k \geq 2$

$$\frac{\|(\mathbf{W} - \mathbf{I})(\mathbf{x}^{(k+1)} - \mathbf{x}_*)\|}{\|(\mathbf{W} - \mathbf{I})(\mathbf{x}^{(k-1)} - \mathbf{x}_*)\|} \leq w_0 \|\mathbf{W}\|, \quad (4)$$

and w_0 is bounded by $\|\mathbf{W}\|$ with $w_0 = \|\mathbf{W}\|$ if and only if $\lambda_{\max}(\mathbf{W}) = -\lambda_{\min}(\mathbf{W})$.

To begin understanding this result, we provide a geometric interpretation of w_0 . While the expression in (3) is rather complicated, it actually follows from a geometric problem. Assume P is an arbitrary point in the xy -plane with y -coordinate equal to 1 and Q is a point on the circle centered at $C = (0, \frac{\lambda_{\max}(\mathbf{W}) + \lambda_{\min}(\mathbf{W})}{2})$ with radius $\frac{\lambda_{\max}(\mathbf{W}) - \lambda_{\min}(\mathbf{W})}{2}$. Let O be the origin, then w_0 is an upper bound on the largest possible $\sin \angle(OPQ)$ formed as P traverses along the line $y = 1$ and Q traverses along the circle. A visualization of this set-up is given in Figure 1. To understand how this geometric object relates to (3), we first note

$$\angle(OPQ) \leq \angle(CPQ) + \angle(OPC). \quad (5)$$

Let $R = (0, 1)$ and assume $|PR| = 1/a$, then

$$\sin \angle(CPQ) \leq \frac{|QC|}{|CP|} = \frac{|\lambda_{\max}(\mathbf{W}) - \lambda_{\min}(\mathbf{W})|a}{\sqrt{4 + (2 - \lambda_{\max}(\mathbf{W}) - \lambda_{\min}(\mathbf{W}))^2 a^2}}. \quad (6)$$

In addition,

$$\begin{aligned} \angle(OPC) &= |\angle(OPR) - \angle(CPR)| \\ &= \left| \tan^{-1} \frac{|OR|}{|PR|} - \tan^{-1} \frac{|CR|}{|PR|} \right| \\ &= \left| \tan^{-1}(a) - \tan^{-1} \left(\left(1 - \frac{\lambda_{\max}(\mathbf{W}) + \lambda_{\min}(\mathbf{W})}{2}\right)a \right) \right|. \end{aligned}$$

Combining these inequalities we have

$$\begin{aligned} \angle(OPQ) &\leq \sin^{-1} \left(\frac{|\lambda_{\max}(\mathbf{W}) - \lambda_{\min}(\mathbf{W})|a}{\sqrt{4 + (2 - \lambda_{\max}(\mathbf{W}) - \lambda_{\min}(\mathbf{W}))^2 a^2}} \right) \\ &\quad + \left| \tan^{-1}(a) - \tan^{-1} \left(\left(1 - \frac{\lambda_{\max}(\mathbf{W}) + \lambda_{\min}(\mathbf{W})}{2}\right)a \right) \right|. \end{aligned}$$

Furthermore, for any a and its associated P , we could choose Q such that this upper bound is obtained by making (5) and (6) tight. In particular, Q is chosen such that PQ is tangent to the circle, making $\angle(PQC) = \pi/2$ and (6) hold with equality, and \vec{PC} is contained inside the cone defined by \vec{PO} and \vec{PQ} , as visualized in Figure 1. As a result, w_0 is the largest possible value of $\sin \angle(OPQ)$.

The following Proposition shows the improvement ratio (4) in Theorem 1 is an equality in the special case where \mathbf{W} is scalar.

Proposition 2 (A special case of a tight bound). *If \mathbf{W} is a scalar matrix and $AA(1)$ is initialized in a particular fashion, with \mathbf{x}_0 and \mathbf{x}_1 independently initialized, then (4) is an equality and $w_0 = \|\mathbf{W}\|/\sqrt{2} - \|\mathbf{W}\|$.*

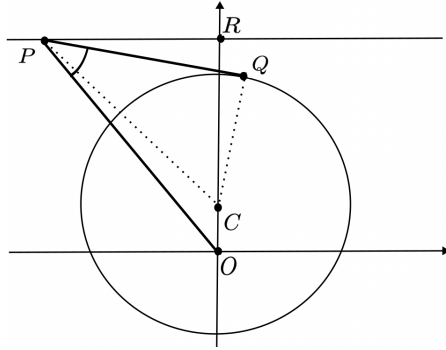


Figure 1: Visualization of w_0 defined in (3). It represents the sine of the largest possible angle $\angle(OPQ)$ formed as P traverses along the line $y = 1$ and Q traverses along the circle.

Theorem 1 implies that the r -linear convergence factor of $AA(m)$ is at most $\|\mathbf{W}\|$, which is the r -linear convergence factor of the fixed-point iteration. The theorem also implies provided $\lambda_{\max}(\mathbf{W}) \neq -\lambda_{\min}(\mathbf{W})$ the convergence factor is strictly smaller. We extend this result below by showing that if $m \geq 2$ the convergence factor of $AA(m)$ is always better than that of the fixed-point method.

Proposition 3 (Improved r -linear convergence factor). *If either $m \geq 2$ or $\lambda_{\max}(\mathbf{W}) \neq -\lambda_{\min}(\mathbf{W})$, then the r -linear convergence factor of $AA(m)$ is strictly smaller than $\|\mathbf{W}\|$ which is the r -linear convergence factor of the fixed-point iteration. If on the other hand $m = 1$ and $\lambda_{\max}(\mathbf{W}) = -\lambda_{\min}(\mathbf{W})$, then the convergence factor of $AA(m)$ may be $\|\mathbf{W}\|$.*

3.2 A Helpful Reformulation of Anderson Acceleration

The proofs of the above results require intricate geometric estimates. Nevertheless, they become simpler by the following reformulation of the Anderson acceleration procedure. To present our equivalent reformulation of $AA(m)$, we may assume without loss of generality $\mathbf{a} = \mathbf{0}$ and as a result $\mathbf{x}_* = \mathbf{0}$. Let $\tilde{\mathbf{x}}^{(k)} = q(\mathbf{x}^{(k)}) - \mathbf{x}^{(k)}$, then $AA(m)$ updates $\tilde{\mathbf{x}}$ iteratively as follows:

1. Let $\tilde{\mathbf{y}}^{(k+1)}$ be the point on the subspace spanned by $\tilde{\mathbf{x}}^{(k-m_k)}, \dots, \tilde{\mathbf{x}}^{(k)}$ with the smallest norm, $\|\tilde{\mathbf{y}}^{(k)}\|^2$.
2. $\tilde{\mathbf{x}}^{(k+1)} = q(\tilde{\mathbf{y}}^{(k+1)})$.

The equivalency of the first step of the reformulated procedure follows from the definition of $AA(m)$. By the definition of $\alpha_j^{(k)}$, we have

$$\tilde{\mathbf{y}}^{(k+1)} = \sum_{j=k-m_k}^k \alpha_j^{(k)} \tilde{\mathbf{x}}^{(j)} = \sum_{j=k-m_k}^k \alpha_j^{(k)} (q(\mathbf{x}^{(j)}) - \mathbf{x}^{(j)}).$$

The equivalency of the second is derived as follows:

$$\begin{aligned}
\tilde{\mathbf{x}}^{(k+1)} &= (q - \mathbf{I})\mathbf{x}^{(k+1)} \\
&= (q - \mathbf{I})\left(\sum_{j=k-m_k}^k \alpha_j^{(k)} q(\mathbf{x}^{(j)})\right) \\
&= (q - \mathbf{I})q\left(\sum_{j=k-m_k}^k \alpha_j^{(k)} (\mathbf{x}^{(j)})\right) \\
&= q(q - \mathbf{I})\left(\sum_{j=k-m_k}^k \alpha_j^{(k)} \mathbf{x}^{(j)}\right) \\
&= q\left(\sum_{j=k-m_k}^k \alpha_j^{(k)} (q - \mathbf{I})\mathbf{x}^{(j)}\right) = q(\tilde{\mathbf{y}}^{(k+1)}),
\end{aligned}$$

where we use the fact $q(\mathbf{x}) = \mathbf{W}\mathbf{x}$.

The compactness of this reformulation removes the discussion of the coefficients, $\alpha_j^{(k)}$, which often occurs in discussions of Anderson acceleration. Thus, with this reformulation we do not need to discuss the boundedness of the coefficients directly. Additionally, this simplification aids the geometric arguments we present which are similar in nature to the discussion provided in Section 3.1. Due to the technical nature of these geometric arguments and the use of graphics as beneficial aids to make the logic of the proofs clear, we present the full proof of Theorem 1 in the supplementary materials.

3.3 Nonlinear Operator

Moving beyond linear operators, we now assume q is nonlinear and has a first-order Taylor expansion at the fixed-point \mathbf{x}_* with symmetric Jacobian $\nabla q(\mathbf{x}_*)$ having operator norm less than one. Let $\mathbf{W} := \nabla q(\mathbf{x}_*)$, then $q(\mathbf{x})$ is locally approximated at \mathbf{x}_* by its first-order Taylor expansion $q(\mathbf{x}_*) + \mathbf{W}(\mathbf{x} - \mathbf{x}_*)$. As a result of this local approximation, the fixed-point iteration has a local r -linear convergence factor of $\|\mathbf{W}\|$, and using our prior analysis we prove a modified version of AA(m) bests the local convergence of the fixed-point iteration.

The modified version of AA(m) we consider for this setting adds an additional bounding constraint on the coefficients $\alpha_j^{(k)}$. Thus, at each iteration, rather than solving (2), the following model is solved

$$\min_{\sum_{j=k-m_k}^k \alpha_j^{(k)} = 1, |\alpha_j^{(k)}| \leq C_0} \left\| \sum_{j=k-m_k}^k \alpha_j^{(k)} (q(\mathbf{x}^{(j)}) - \mathbf{x}^{(j)}) \right\|, \quad (7)$$

where $C_0 > 0$ is a fixed constant. We refer to AA(m) with (2) replaced by (7) as modified AA(m).

With this slight alteration, we prove the local convergence of modified AA(m) is superior to that of the fixed-point iteration.

Theorem 4 (Local convergence rate of modified AA(m) for nonlinear operators). *Assume \mathbf{x}_* is a fixed-point of q with $\mathbf{W} := \nabla q(\mathbf{x}_*)$ symmetric, $\|\mathbf{W}\| < 1$, and $\lambda_{\max}(\mathbf{W}) \neq -\lambda_{\min}(\mathbf{W})$. Then there exists a constant C'_0 such that when $C_0 > C'_0$ and $\mathbf{x}^{(1)}$ is sufficiently close to \mathbf{x}_* , modified AA(m) converges with local r -linear convergence factor no larger than $\sqrt{w_0\|\mathbf{W}\|}$ with $w_0 < \|\mathbf{W}\|$.*

Since the local r -linear convergence factor of the fixed-point iteration is $\|\mathbf{W}\|$, Theorem 4 implies modified AA(m) outperforms the fixed-point iteration. The proof of Theorem 4 is based on a similar argument to the proof of Theorem 1 and leverages the local first-order approximation of q .

3.3.1 Tyler’s M-estimator

Tyler’s M-estimator (TME) (Tyler, 1987a) is a popular method for robust covariance estimation, that is, for estimation of the covariance matrix in a way that is resistant to the influence of outliers or deviations from the assumed statistical model. This estimator is obtainable through fixed-point iterations, and we show one such formulation satisfies the symmetry assumption in Theorem 4. TME provides an important instance of a nonlinear operator to test AA, and we compare the performance of AA to the fixed-point iterations later in Section 4.

Given a data set $\{\mathbf{x}_i\}_{i=1}^n \subset \mathbb{R}^p$, the standard fixed-point iteration to compute Tyler’s M-estimator is

$$\Sigma^{(k+1)} = G(\Sigma^{(k)}) := \frac{p}{n} \sum_{i=1}^n \frac{\mathbf{x}_i \mathbf{x}_i^T}{\mathbf{x}_i^T \Sigma^{(k)-1} \mathbf{x}_i}, \quad (8)$$

subject to the constraint $\text{tr}(\Sigma^{(k+1)}) = p$. Kent and Tyler (1988) established the uniqueness and existence of the underlying fixed-point of (8) and its constraint, which defines the TME, along with proving convergence. Their theory holds under a natural geometric condition that avoids concentration on lower-dimensional subspaces, namely, any linear subspace of \mathbb{R}^p of dimension $1 \leq d \leq p - 1$ contains less than nd/p of the data points. Franks and Moitra (2020) established the linear convergence of (8). TME can be interpreted as the maximum likelihood estimator of the shape matrix of the angular central Gaussian distribution (Tyler, 1987b) and of the generalized elliptical distribution (Frahm and Jaekel, 2010). Furthermore, for data i.i.d. sampled from a continuous elliptical distribution, TME emerges as the “most robust” covariance estimator as n approaches infinity (Tyler, 1987a). The practical utility of TME found successful applications across various domains (Frahm and Jaekel, 2007; Chen et al., 2011; Ollila and Koivunen, 2003; Ollila and Tyler, 2012).

An alternative iterative procedure for solving for the TME was introduced by Zhang et al. (2016).

They showed an equivalent fixed-point iteration for TME is given by

$$\mathbf{w}^{(k)} = F(\mathbf{w}^{(k-1)}), \quad (9)$$

where $F : \mathbb{R}^n \rightarrow \mathbb{R}^n$ and the j -th component of F is given by

$$F_j(\mathbf{w}) = -\log \left(\mathbf{x}_j^T \left(\frac{p}{n} \sum_{i=1}^n e^{w_i} \mathbf{x}_i \mathbf{x}_i^T \right)^{-1} \mathbf{x}_j \right). \quad (10)$$

One can quickly verify the equivalence by letting

$$\Sigma^{(k)} = \frac{p}{n} \sum_{i=1}^n e^{w_i^{(k)}} \mathbf{x}_i \mathbf{x}_i^T. \quad (11)$$

Then (10) implies

$$w_j^{(k+1)} = -\log(\mathbf{x}_j^T \Sigma^{(k)-1} \mathbf{x}_j), \quad (12)$$

and from these equations one can obtain the standard fixed-point iteration. Notably, however, though these iterations are equivalent, the standard iterative procedure fails to have a symmetric Jacobian at fixed-points while the alternative procedure does. The next lemma proves this fact.

Lemma 5. *Let \mathbf{w}^* be a fixed-point of (9). Then, $\nabla F(\mathbf{w}^*)$ is symmetric.*

Since our numerical results directly apply this lemma and its proof is short we include it here.

Proof. At the fixed-point \mathbf{w}^* we have

$$w_j^* = -\log \left(\mathbf{x}_j^T \left(\frac{p}{n} \sum_{i=1}^n e^{w_i^*} \mathbf{x}_i \mathbf{x}_i^T \right)^{-1} \mathbf{x}_j \right)$$

which implies

$$\mathbf{x}_j^T \left(\frac{p}{n} \sum_{i=1}^n e^{w_i^*} \mathbf{x}_i \mathbf{x}_i^T \right)^{-1} \mathbf{x}_j = e^{-w_j^*}. \quad (13)$$

From (11), (12), and (13) it follows

$$e^{w_j^*} = \frac{1}{\mathbf{x}_j^T \Sigma^{*-1} \mathbf{x}_j}.$$

Therefore,

$$\frac{d}{dw_i} F_j(\mathbf{w}^*) = \frac{\mathbf{x}_j^T \Sigma^{*-1} \left(\frac{p}{n} e^{w_i^*} \mathbf{x}_i \mathbf{x}_i^T \right) \Sigma^{*-1} \mathbf{x}_j}{\mathbf{x}_j^T \Sigma^{*-1} \mathbf{x}_j} = e^{w_j^*} \mathbf{x}_j^T \Sigma^{*-1} \left(\frac{p}{n} e^{w_i^*} \mathbf{x}_i \mathbf{x}_i^T \right) \Sigma^{*-1} \mathbf{x}_j$$

from which we see $\frac{d}{dw_i} F_j(\mathbf{w}^*) = \frac{d}{dw_j} F_i(\mathbf{w}^*)$ for all i and j . □

3.4 Discussion of Results

Our work establishes an upper bound on the r -linear convergence factor of AA(m) which we show in many cases to be strictly less than the convergence factor of the fixed-point iteration. This result is a new addition to the literature because we directly show AA has a better rate which prior works have not clearly demonstrated (Evans et al., 2020; De Sterck and He, 2022; Pollock and Rebholz, 2021; Pollock et al., 2019) as attested to by the quote of De Sterck and He referenced in the introduction.

Our analysis studied the improvement of AA over every pair of iterations, and we see the estimates we derived can be tight. In Section 4, we show in our numerical experiments our estimation in (4) is usually tight for AA(1) for all k . In practice, we observe the improvement factor varies over iterations, see Figures 2 and 4, which results in a smaller r -linear convergence factor asymptotically. Additionally, we have noted the improvement factor appears to depend upon m ; therefore, we conjecture our estimation of the r -linear convergence factor could be improved by investigating the improvement of AA over more consecutive iterations. We also expect faster convergence rates when $m \geq 2$, improving from our current estimation that is independent of m . For example, Proposition 3 already shows that there are some settings where AA(m) with $m \geq 2$ has an improved convergence factor over $m = 1$, and existing results (Scieur, 2019) establish the convergence factor when m is infinite, which is numerically smaller than our rate of $\sqrt{w_0 \|\mathbf{W}\|}$.

As a closing remark, in practice it is common to apply a damping technique in AA(m), that is, instead of (3), the next iterate is updated as

$$\mathbf{x}^{(k+1)} = \beta \sum_{j=k-m_k}^k \alpha_j^{(k)} q(\mathbf{x}^{(j)}) + (1 - \beta) \sum_{j=k-m_k}^k \alpha_j^{(k)} \mathbf{x}^{(j)}$$

for some $\beta \in [0, 1]$. If this technique is applied, similar results to ours can be obtained. For example, Theorem 1 and Proposition 3 hold by replacing \mathbf{W} with $\beta\mathbf{W} + (1 - \beta)\mathbf{I}$.

4 Simulations

We investigate our theoretical results with numerical experiments on symmetric linear and nonlinear operators in Sections 4.1 and 4.2 respectively. Our numerical experiments provide empirical support for our theoretical results and demonstrate the effectiveness of Anderson acceleration for Tyler’s M-estimation.

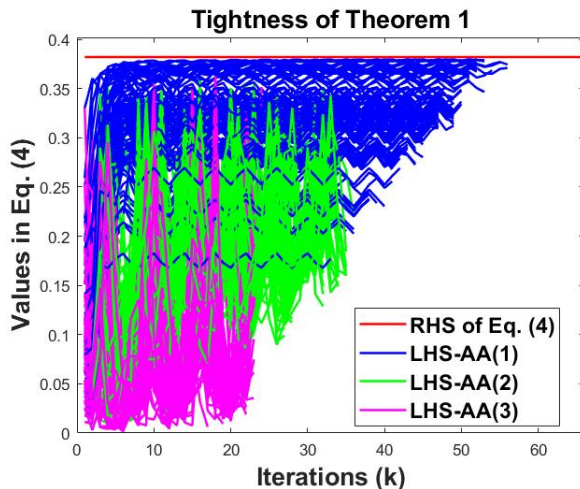


Figure 2: Presents the left-hand side of (4) for all iterations $k \geq 2$ for one hundred random initializations of AA(1), AA(2), and AA(3) with $q_1(\mathbf{x}) = \mathbf{W}_1\mathbf{x}$ where $\mathbf{W}_1 = \text{Diag}([-0.07, 0.62, -0.55, -0.6, 0.15])$; LHS-AA(m) denotes the value of the left-hand side of (4) for the iterates of AA(m) for each random initialization while the red line shows the constant right-hand side of (4).

4.1 Linear operators

In this section, we conduct numerical experiments on linear operators $q(\mathbf{x}) = \mathbf{W}\mathbf{x} + \mathbf{a}$, where \mathbf{W} is symmetric and $\|\mathbf{W}\| < 1$, and verify the tightness of the upper bound on the r -linear convergence factor proven in Theorem 1. We present two experiments; the first verifies the tightness of (4); the second displays the upper bound on the r -linear convergence factor for AA(m).

For experiment one, we define $q_1(\mathbf{x}) := \mathbf{W}_1\mathbf{x}$ where $\mathbf{W}_1 = \text{Diag}([-0.07, 0.62, -0.55, -0.6, 0.15])$. We compute the fixed-point of q_1 with AA(m) for $m = 1, 2$, and 3 and check inequality (4) for the iterates generated by AA(m) for one hundred random initializations of each algorithm. Each instance of AA(m) terminated once the fixed-point error, i.e., $\|q_1(\mathbf{x}) - \mathbf{x}\|$, was less than 10^{-12} . The random initial vectors for AA(m) had entries drawn from a standard normal. Figure 2 displays the result of the numerical experiment.

We observe in Figure 2 that the value of the left-hand side of (4) was always bounded by the right-hand side. The set of iterates generated by AA(1) obtained the minimum gap of 0.0024 between the left and right-hand sides of (4). In relative terms, the minimum gap was 0.62% of the value of the right-hand side which strongly supports the tightness of the inequality.

Our second experiment demonstrates the upper bound on the r -linear convergence factor for AA(m)

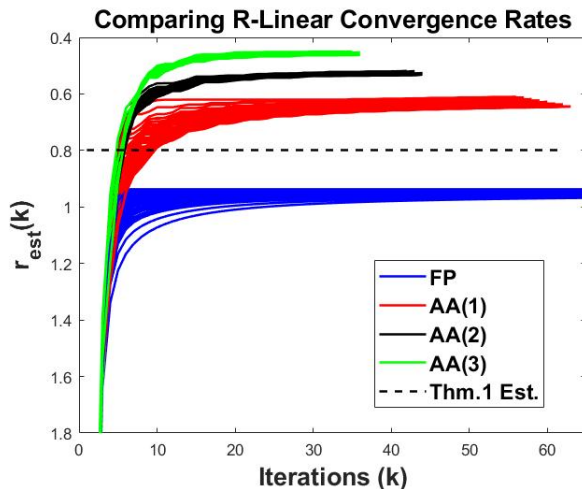


Figure 3: Displays the estimated r-linear convergence factors for FP, AA(1), AA(2), and AA(3) for the linear operator $q_2(\mathbf{x}) = \mathbf{W}_2\mathbf{x}$ for one hundred random initializations of each method. The dashed line is the upper-bound on the r-linear convergence factor from Theorem 1.

provided by Theorem 1. For this experiment, we randomly generated $\mathbf{W}_2 \in \mathcal{S}^{500 \times 500}$ with all but the smallest eigenvalue drawn uniformly at random between -0.9 and 0.9; the smallest eigenvalue was chosen to be -0.95. We applied the fixed-point iteration (FP), AA(1), AA(2), and AA(3) to solve $q_2(\mathbf{x}) := \mathbf{W}_2\mathbf{x}$ from one hundred random initializations. We used the same initialization process and termination criteria as in the first experiment. At each iterate k , we estimated the r-linear convergence factor as

$$r_{est}(k) := \max_{n \geq k} \|\mathbf{x}_* - \mathbf{x}^{(n)}\|^{1/n}. \quad (14)$$

Figure 3 displays the result of the numerical experiment. The figure shows that the predicted bound on the r-linear convergence factor is both an upper bound on the performance of AA(m) and is a strict lower bound on the performance of the fixed-point iteration. Additionally, it shows that the r-linear convergence factors for AA(m) depends on the initialization, as observed in the literature, and that the convergence factor improves as m increases.

4.2 Nonlinear operator

For our nonlinear operator experiments we investigate Anderson acceleration applied to Tyler’s M-estimation described in Section 3.3.1. For our experiments we utilized two data models:

Data Model 1: Letting $(S_p)_{ij} = (0.7)^{|i-j|}$, data points were generated as $\mathbf{x}_i = \mathbf{S}_p^{1/2}\boldsymbol{\zeta}$ where $\boldsymbol{\zeta}_i \sim \mathcal{N}(0, 1)$; we generated 110 data points with $\mathbf{x}_i \in \mathbb{R}^{100}$; see Section 7.1 of Goes et al. (2020) for a full description of this model.

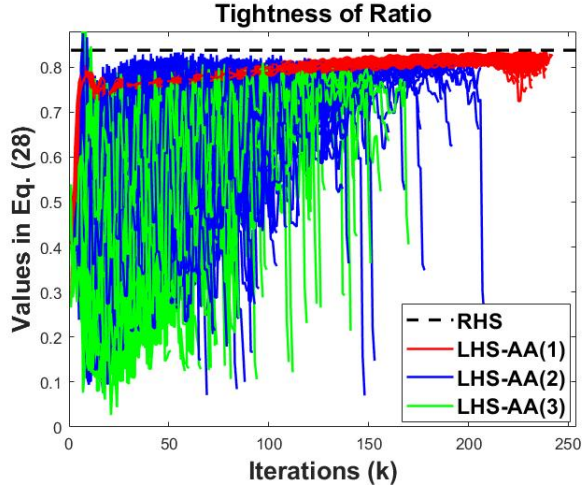


Figure 4: Displays the value of the LHS of (28) for iterates generated by AA(m) for one hundred random initializations for an instance of Data Model 1. LHS-AA(m) denotes the value of the LHS of (28) for the iterates of AA(m) for each random initialization; the black dotted line is the RHS of (28).

Data Model 2: This model is an inlier-outlier model containing 997 data points in \mathbb{R}^{100} . The data matrix \mathbf{X} , whose columns form the data set $\{\mathbf{x}_i\}_{i=1}^n$, was formed as

$$\mathbf{X} = \begin{pmatrix} \text{randn}(n_0, D) \cdot \text{randn}(D, D) \\ [\text{randn}(n_1, d)/\sqrt{d} \mid \mathbf{0}] \end{pmatrix}^\top,$$

where $n_0 = 500$, $n_1 = 497$, $D = 100$, $d = 50$, and $\text{randn}(m, n)$ forms an m -by- n matrix with entries drawn from a standard normal.

We begin with numerical tests on Data Model 1. Our first experiment compared the alternative TME fixed-point iteration to AA(m) applied to (10) for an instance of Data Model 1 to verify the theoretical results while the second and third experiments display the superior performance of AA(m) over the standard TME fixed-point method.

In the first experiment, each method was randomly initialized one hundred times, and all methods were terminated once the fixed-point error was less than 10^{-12} . To fairly estimate the r-linear convergence factor of the methods, we first computed the unique solution to the TME having trace equal to $p = 100$. The estimates of the r-linear convergence factors for each method were then computed from (14) by using (11) to transform each vector iterate, $\mathbf{w}^{(k)}$, into a matrix which was then scaled to have trace equal to p .

The reason for this estimation of the r-linear convergence factor follows from the scale-invariance of the TME, that is, F has multiple fixed-points: if \mathbf{w}_* is a fixed-point then $\mathbf{w}_* + \mathbf{c}$, with constant

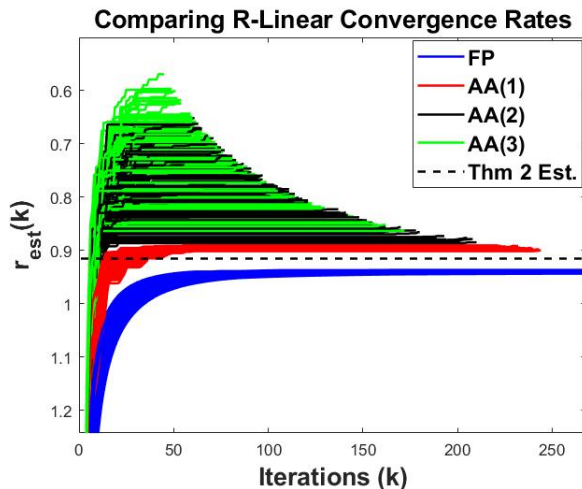


Figure 5: Displays the estimated r-linear convergence rates of AA(m) applied to (10) and the alternative TME fixed-point iteration for one hundred random initializations of the methods for an instance of Data Model 1. The dashed line is the upper-bound on the r-linear convergence factor given by Theorem 2.

vector \mathbf{c} , is a fixed-point. The scale-invariance also causes $\mathbf{W} := \nabla F(\mathbf{w}_*)$, with \mathbf{w}_* a fixed-point of (10), to have an eigenvalue of 1 with a constant eigenvector. As a result, we use the second largest eigenvalue of \mathbf{W} to calculate the right-hand side of (28) and the upper bound on the r-linear convergence factor for AA(m). We observe this generates accurate bounds in our experiments.

Figures 4 and 5 present the results of the numerical experiment performed on Data Model 1. We observe in Figure 4 the right-hand side of (28) serves as an upper bound on the improvement ratio. Our theory predicts the bound will hold for all iterates sufficiently close to a solution and the figure supports this. Figure 5 clearly presents that the upper bound on the r-linear convergence factor given by Theorem 4 holds; AA(m) for $m = 1, 2$, and 3 all out-perform the estimate while the fixed-point scheme given by (10) has an r-linear factor larger than the given estimate.

We next present two numerical tests which compare the computational expense and performance of AA(m) and the standard TME fixed-point iteration on Data Model 1. We utilized the standard TME fixed-point iteration over the alternative approach when comparing computational time and cost because we found the fixed-point iteration given by (8) outperformed (10) for these measures. As before, we solved ten different instantiations of Data Model 1 from ten different random initializations of our methods. The two settings of Data Model 1 we considered were $(p, n) = (100, 110)$ and $(p, n) = (200, 210)$. Each method ran until the fixed-point error was less than or equal to 10^{-12} . Figures 6 and 7 display the results of the numerical experiments. From the figures, we see that in all of the tests AA(m) required less iterations to compute a solution to the desired tolerance. For the

setting $(p, n) = (100, 110)$, AA(3) always obtained a solution faster than the fixed-point iteration while AA(2) computed a solution slower one time in all of the one hundred experiments. The results were similar for $(p, n) = (200, 210)$. In this setting, AA(2) and AA(3) computed solutions faster than the fixed-point approach in all tests, and the fixed-point iteration only computed a solution faster than AA(1) in two tests. Thus, these experiments demonstrate that Anderson acceleration provides a powerful method for solving the TME and can significantly outperform the standard fixed-point schemes, besting these methods in both iteration and computational complexity in a vast majority of our test cases.

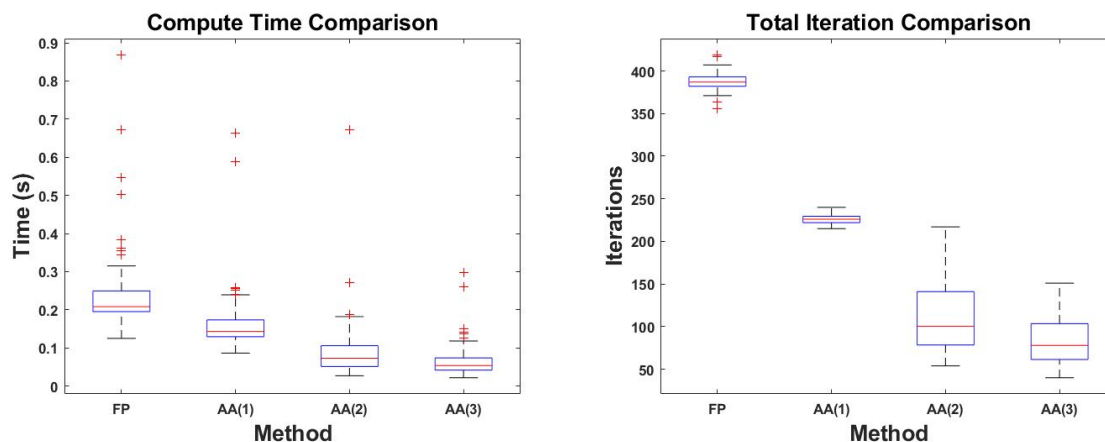


Figure 6: Displays boxplots for the computational time and total iterations required to solve TME with the standard TME fixed-point iteration (FP) and AA(m) applied to the alternative TME fixed-point iteration for Data Model 1 with $(p, n) = (100, 110)$.

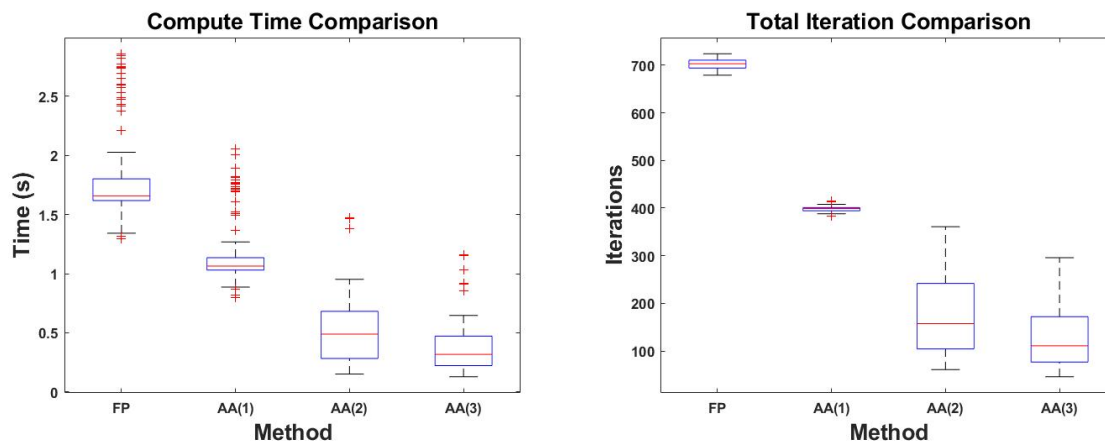


Figure 7: Displays boxplots for the computational time and total iterations required to solve TME with the standard TME fixed-point iteration (FP) and AA(m) applied to the alternative TME fixed-point iteration for Data Model 1 with $(p, n) = (200, 210)$.

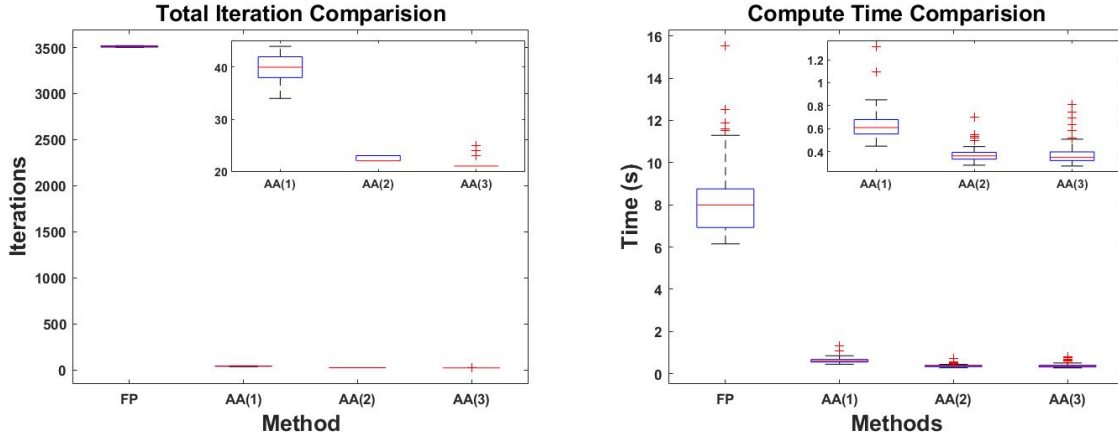


Figure 8: Presents a box-plot of the iterations and time required for each method to compute a solution for Tyler’s M-estimation with Data Model 2; FP refers to the fixed-point iteration (8) with scaled iterate to have trace equal to p while AA(m) references AA(m) applied to (10).

Data Model 2 was used in our second set of experiments. We solved ten different instantiations of the model with ten different random initializations of each method for a total of one hundred implementations of each method. All algorithms were terminated when the fixed-point error was less than 10^{-12} .

The results of the numerical tests are presented in Figure 8 with a set of box-plots. The figure clearly demonstrates AA(1), AA(2), and AA(3) computed solutions to TME faster than the standard fixed-point iteration for all experiments with AA(m) converging nearly ten-times faster in every test. The comparison for Data Model 2 was even more striking than for Data Model 1. In this inlier-outlier setting, the fixed-point method was completely outclassed by AA; therefore, this suggests the possibility Anderson acceleration can prove to be a great benefit in settings where the standard fixed-point approach exhibits slow linear convergence.

Besides investigating the computational advantage of AA(m), we further validated the strength of our theory in the non-linear setting. Figure 9 compares the r-linear convergence factor of AA(m) compared to the standard TME fixed-point iteration and displays the bound in (28) for the experiments displayed in Figure 8. Figure 8 clearly demonstrated Anderson acceleration vastly decreased the compute time, and the right panel in Figure 9 gives some evidence as to why. The r-linear convergence factors of AA(2) and AA(3) in the one hundred experiments were approximately 0.4 while the r-linear convergence factor of the standard TME fixed-point iteration was about one. As discussed in Section 3.4, we note the closeness of the estimate of the r-linear convergence factor to the fixed-point method’s rate suggests our theory can further be refined to achieve a better bound. This might be achieved by investigating the improvement of AA(m) over more iterations than currently investigated in our analysis.

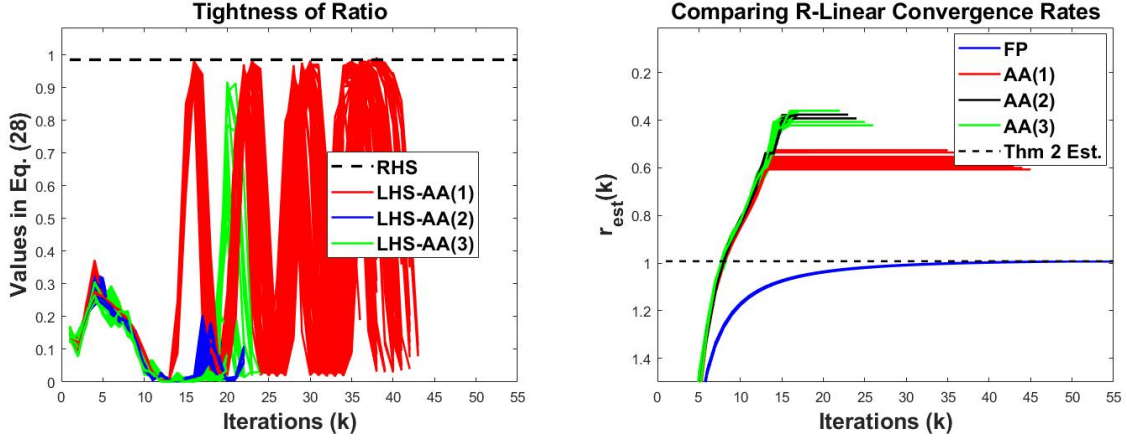


Figure 9: Displays the results of the hundred random experiments conducted on Data Model 2. The panel on the left displays the value of the LHS of (28) for iterates generated by AA(m) applied to (10). The panel on the right displays the estimated r-linear convergence rates of AA(m) applied to the alternative TME fixed-point iteration. The dashed line is the upper-bound on the r-linear convergence factor given by Theorem 2.

5 Technical Proofs

We present here the proofs of the results stated in Section 3.

5.1 Proof of Theorem 1

Proof. As described in Section 3.2, we may assume without loss of generality $\mathbf{a} = \mathbf{0}$ and $\mathbf{x}_* = \mathbf{0}$ and reformulate AA(m) as the following iterative process:

1. Let $\tilde{\mathbf{y}}^{(k+1)}$ be the point on the subspace spanned by $\tilde{\mathbf{x}}^{(k-m_k)}, \dots, \tilde{\mathbf{x}}^{(k)}$ with the smallest norm, $\|\tilde{\mathbf{y}}^{(k)}\|^2$.
2. $\tilde{\mathbf{x}}^{(k+1)} = q(\tilde{\mathbf{y}}^{(k+1)})$.

where $m_k := \min(m, k)$ and we assumed in our derivation of the reformulation $\tilde{\mathbf{x}}^{(k)} = q(\mathbf{x}^{(k)}) - \mathbf{x}^{(k)}$. We first verify (4). We begin by noting (4) is equivalent to

$$\frac{\|\tilde{\mathbf{x}}^{(k+1)}\|}{\|\tilde{\mathbf{x}}^{(k-1)}\|} \leq w_0 \|\mathbf{W}\|.$$

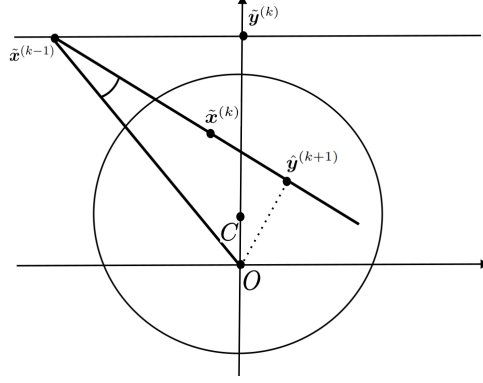


Figure 10: A visualization of $\tilde{\mathbf{x}}^{(k-1)}$, $\tilde{\mathbf{x}}^{(k)}$, $\tilde{\mathbf{y}}^{(k)}$, and $\hat{\mathbf{y}}^{(k+1)}$. The ball with center C represents the region defined by Lemma 6 showing the possible values of $\mathbf{W}\tilde{\mathbf{y}}^{(k)}$.

Since $\tilde{\mathbf{x}}^{(k+1)} = q(\tilde{\mathbf{y}}^{(k+1)})$ by Step 2 it follows $\|\tilde{\mathbf{x}}^{(k+1)}\| \cdot \|\mathbf{W}\|^{-1} \leq \|\tilde{\mathbf{y}}^{(k+1)}\|$. Therefore, to prove (4) it is sufficient to show

$$\frac{\|\tilde{\mathbf{y}}^{(k+1)}\|}{\|\tilde{\mathbf{x}}^{(k-1)}\|} \leq w_0. \quad (15)$$

We now demonstrate this relationship holds. Let $\hat{\mathbf{y}}^{(k+1)}$ be the projection of the origin to the line connecting $\tilde{\mathbf{x}}^{(k-1)}$ and $\tilde{\mathbf{x}}^{(k)}$, thereby making it a linear combination of $\tilde{\mathbf{x}}^{(k-1)}$ and $\tilde{\mathbf{x}}^{(k)}$. Then by the definition of $\tilde{\mathbf{y}}^{(k+1)}$ in Step 1 we have

$$\|\hat{\mathbf{y}}^{(k+1)}\| \geq \|\tilde{\mathbf{y}}^{(k+1)}\| \quad (16)$$

and

$$\frac{\|\hat{\mathbf{y}}^{(k+1)}\|}{\|\tilde{\mathbf{x}}^{(k-1)}\|} = \sin \angle(\mathbf{O}\tilde{\mathbf{x}}^{(k-1)}\hat{\mathbf{y}}^{(k+1)}) = \sin \angle(\mathbf{O}\tilde{\mathbf{x}}^{(k-1)}\tilde{\mathbf{x}}^{(k)}). \quad (17)$$

By (16) and (17) it follows, if we prove $\sin \angle(\mathbf{O}\tilde{\mathbf{x}}^{(k-1)}\tilde{\mathbf{x}}^{(k)}) \leq w_0$, then we will have proven our claim. To help bound the sine of this angle, we introduce the following lemma:

Lemma 6. For any symmetric matrix \mathbf{W} , $\mathbf{W}\mathbf{x}$ lies in the ball centered at $(\lambda_{\max}(\mathbf{W}) + \lambda_{\min}(\mathbf{W}))\mathbf{x}/2$ with radius $(\lambda_{\max}(\mathbf{W}) - \lambda_{\min}(\mathbf{W}))\|\mathbf{x}\|/2$.

Proof. Given any $\mathbf{W} \in \mathcal{S}^{n \times n}$ and $\mathbf{x} \in \mathbb{R}^n$, we see

$$\begin{aligned} \left\| \mathbf{W}\mathbf{x} - \frac{1}{2}(\lambda_{\max}(\mathbf{W}) + \lambda_{\min}(\mathbf{W}))\mathbf{x} \right\| &\leq \left\| \mathbf{W} - \frac{1}{2}(\lambda_{\max}(\mathbf{W}) + \lambda_{\min}(\mathbf{W}))\mathbf{I} \right\| \cdot \|\mathbf{x}\| \\ &= \frac{1}{2}(\lambda_{\max}(\mathbf{W}) - \lambda_{\min}(\mathbf{W}))\|\mathbf{x}\|. \end{aligned}$$

□

We now utilize a geometric argument. First, we note without loss of generality we may assume $\tilde{\mathbf{y}}^{(k)} = [0, 1, 0, \dots, 0]$. Then following the definition of $\tilde{\mathbf{y}}^{(k)}$, $\tilde{\mathbf{x}}^{(k-1)} - \tilde{\mathbf{y}}^{(k)}$ is perpendicular to $\tilde{\mathbf{y}}^{(k)}$, and $\tilde{\mathbf{x}}^{(k-1)}$ must lie on the hyperplane through the point $(0, 1, 0, \dots, 0)$ with normal vector being the second standard basis vector in \mathbb{R}^n . Note, we may assume this by applying a unitary transformation and scaling all points $\tilde{\mathbf{x}}^{(j)}$, $j = k - m_k, \dots, k$, which form $\tilde{\mathbf{y}}^{(k)}$. Furthermore, by unitary transformation we may also assume $\tilde{\mathbf{x}}^{(k-1)} - \tilde{\mathbf{y}}^{(k)}$ is parallel to the first standard basis vector in \mathbb{R}^n . A geometric representation of our transformed problem, presenting the relationship between $\tilde{\mathbf{x}}^{(k-1)}$, $\tilde{\mathbf{x}}^{(k)}$, $\tilde{\mathbf{y}}^{(k)}$, and $\hat{\mathbf{y}}^{(k+1)}$, is given in Figure 10. Using Lemma 6, we denote in Figure 10 all the possible values of $\tilde{\mathbf{x}}^{(k)} = \mathbf{W}\tilde{\mathbf{y}}^{(k)}$, which is given by all the points contained in the ball centered at $C = (\lambda_{\max}(\mathbf{W}) + \lambda_{\min}(\mathbf{W}))\tilde{\mathbf{y}}^{(k)}/2$ with radius

$$r := (\lambda_{\max}(\mathbf{W}) - \lambda_{\min}(\mathbf{W}))\|\tilde{\mathbf{y}}^{(k)}\|/2 = (\lambda_{\max}(\mathbf{W}) - \lambda_{\min}(\mathbf{W}))/2.$$

Our aim is to bound $\angle(\mathbf{O}\tilde{\mathbf{x}}^{(k-1)}\tilde{\mathbf{x}}^{(k)})$, which we realize is maximized when $\tilde{\mathbf{x}}^{(k)}$ is on the sphere centered at C with radius r such that the line connecting $\tilde{\mathbf{x}}^{(k-1)}$ and $\tilde{\mathbf{x}}^{(k)}$ is tangent to the sphere. As a result, the value of $\tilde{\mathbf{x}}^{(k)}$ which maximizes $\angle(\mathbf{O}\tilde{\mathbf{x}}^{(k-1)}\tilde{\mathbf{x}}^{(k)})$ lies in a 2-dimensional plane containing $\tilde{\mathbf{x}}^{(k)}$ and $\tilde{\mathbf{y}}^{(k)}$. A visualization of this setting is depicted in Figure 11. Note, another possible orientation of the figure has C below the x -axis. Then the visualization would be different as the line connecting $\tilde{\mathbf{x}}^{(k-1)}$ and $\tilde{\mathbf{x}}^{(k)}$ will be the other tangent line; however, the argumentation for this setting is analogous and does not alter the derivation of w_0 .

The setting represented by Figure 11 is identical to Figure 1 in Section 3.1, with $P = \tilde{\mathbf{x}}^{(k-1)}$, $R = \tilde{\mathbf{y}}^{(k)}$, $Q = \tilde{\mathbf{x}}^{(k)}$. As a result, the argument presented in Section 3.1 following the statement of Theorem 1 holds and w_0 is as defined in (3). Therefore, following our previous discussion, $\sin \angle(\mathbf{O}\tilde{\mathbf{x}}^{(k-1)}\tilde{\mathbf{x}}^{(k)}) \leq w_0$ for all possible $\tilde{\mathbf{x}}^{(k)}$, i.e., all points inside in the ball specified by Lemma 6, which proves (4).

Since $\|\mathbf{W}\| < 1$, we know the sequence $\{\tilde{\mathbf{x}}^{(k)}\}$ converges to $\mathbf{x}_* = \mathbf{0}$. Using (4), we see the r-linear convergence factor is bounded by $\sqrt{w_0\|\mathbf{W}\|}$. From (4) it follows

$$\|\tilde{\mathbf{x}}^{(k)}\| \leq w_0\|\mathbf{W}\|\|\tilde{\mathbf{x}}^{(k-2)}\| \leq (w_0\|\mathbf{W}\|)^2\|\tilde{\mathbf{x}}^{(k-4)}\| \leq \dots \leq (w_0\|\mathbf{W}\|)^{\lfloor (k-2)/2 \rfloor} \max\left(\|\tilde{\mathbf{x}}^{(0)}\|, \|\tilde{\mathbf{x}}^{(1)}\|\right),$$

and so

$$\rho_{\{\tilde{\mathbf{x}}^{(k)}\}} = \limsup_{k \rightarrow \infty} \|\tilde{\mathbf{x}}^{(k)}\|^{1/k} \leq \lim_{k \rightarrow \infty} \left((w_0\|\mathbf{W}\|)^{\lfloor (k-2)/2 \rfloor} \max\left(\|\tilde{\mathbf{x}}^{(0)}\|, \|\tilde{\mathbf{x}}^{(1)}\|\right) \right)^{1/k} = \sqrt{w_0\|\mathbf{W}\|}.$$

Lastly, we prove $w_0 \leq \|\mathbf{W}\|$, with equality holding if and only if $\lambda_{\max}(\mathbf{W}) = -\lambda_{\min}(\mathbf{W})$. Using our geometric understanding of the problem in Figure 1, we note

$$\sin \angle(OPQ) = \frac{\text{dist}(O, L)}{|OP|},$$

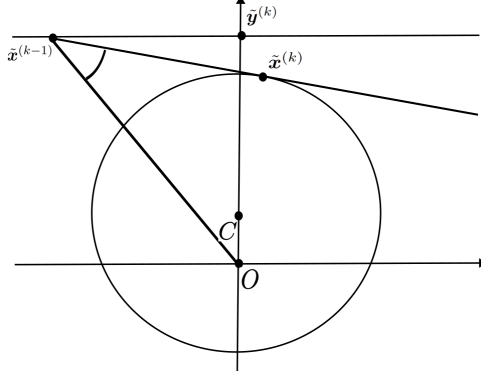


Figure 11: A visualization when $\angle(O\tilde{\mathbf{x}}^{(k-1)}\tilde{\mathbf{x}}^{(k)})$ is at its maximum.

where L represents the line connecting P and Q . Looking at the terms in this ratio we see

$$|OP| \geq |OR| = 1 \quad (18)$$

and

$$\text{dist}(O, L) \leq |OC| + \text{dist}(C, L) = |OC| + |CQ| = \|\mathbf{W}\| \quad (19)$$

and so it follows that $\sin \angle(OPQ) \leq \|\mathbf{W}\|$; therefore, since w_0 is the largest possible $\sin \angle(OPQ)$, we have $w_0 \leq \|\mathbf{W}\|$. From the argument above, $w_0 = \|\mathbf{W}\|$ only when (18) and (19) are equalities, that is, $P = R$ and O, C, Q are collinear. If $C \neq O$, then the collinearity of O, C, Q implies that Q must lie on the y -axis in Figure 1; however, this would violate the required tangency of L with the circle. As a result, $w_0 = \|\mathbf{W}\|$ will only occur in this problem provided $O = C$, i.e., $\lambda_{\min}(\mathbf{W}) + \lambda_{\max}(\mathbf{W}) = 0$. On the other hand, when $\lambda_{\min}(\mathbf{W}) + \lambda_{\max}(\mathbf{W}) = 0$, we have $C = O$ in Figure 1 and the circle has a radius of $\|\mathbf{W}\|$. Let $a \rightarrow \infty$ in (3), i.e., $P = R$ in Figure 1, it follows that $\sin \angle(OPQ) = \|\mathbf{W}\|$; therefore, $w_0 = \|\mathbf{W}\|$. \square

5.2 Proof of Proposition 2

Proof. Let $\mathbf{W} = w\mathbf{I}$ with $|w| < 1$. We define $\tilde{\mathbf{y}}^{(k)}$ and $\tilde{\mathbf{x}}^{(k)}$ as discussed in the proof of Theorem 1 and assume without loss of generality $\tilde{\mathbf{y}}^{(k)} = [0, 1, 0, \dots, 0]$ and that $\tilde{\mathbf{x}}^{(k-1)}$ lies on the hyperplane through the point $(0, 1, 0, \dots, 0)$ with normal vector parallel to the second standard basis vector in \mathbb{R}^n . Given the geometric meaning of w_0 discussed in Section 3.1 and in the proof of Theorem 1, it suggests the circle in Figure 10 has radius 0 and is reduced to a point centered at $C = w\tilde{\mathbf{y}}^{(k)}$, and w_0 is equivalent to finding a point P on the line $y = 1$ such that $\angle(OPC)$ is the largest and O is the origin. Let $R = (0, 1)$ and $|PR| = 1/a$ with $a > 0$. Then,

$$\angle(OPC) = \angle(OPR) - \angle(CPR) = \tan^{-1}(a) - \tan^{-1}((1 - \|\mathbf{W}\|)a),$$

and taking the derivative with respect to a we see the maximum angle is achieved when

$$\frac{1}{1+a^2} = \frac{(1-\|\mathbf{W}\|)}{1+(1-\|\mathbf{W}\|)^2 a^2}, \text{ that is, } a = \frac{1}{\sqrt{1-\|\mathbf{W}\|}}.$$

Then,

$$\begin{aligned} \sin(\angle(OPC)) &= \sin\left(\tan^{-1} \frac{1}{\sqrt{1-\|\mathbf{W}\|}}\right) \cos(\tan^{-1} \sqrt{1-\|\mathbf{W}\|}) \\ &\quad - \cos\left(\tan^{-1} \frac{1}{\sqrt{1-\|\mathbf{W}\|}}\right) \sin(\tan^{-1} \sqrt{1-\|\mathbf{W}\|}) \\ &= \frac{1}{\sqrt{2-\|\mathbf{W}\|}} \frac{1}{\sqrt{2-\|\mathbf{W}\|}} - \frac{\sqrt{1-\|\mathbf{W}\|}}{\sqrt{2-\|\mathbf{W}\|}} \frac{\sqrt{1-\|\mathbf{W}\|}}{\sqrt{2-\|\mathbf{W}\|}} \end{aligned}$$

and therefore $w_0 = \|\mathbf{W}\|/(2-\|\mathbf{W}\|)$.

Next, we show when AA(1) is applied to this problem with a specific initialization that (4) is equality. For this argument, a visualization is provided in Figure 12. Let $\theta^{(k)} = \angle(\tilde{\mathbf{y}}^{(k)} \tilde{\mathbf{x}}^{(k-1)} O)$ and $\theta^{(k+1)} = \angle(\tilde{\mathbf{y}}^{(k+1)} \tilde{\mathbf{x}}^{(k)} O)$. Then,

$$\tan \theta^{(k+1)} = \tan \angle(\tilde{\mathbf{y}}^{(k+1)} \tilde{\mathbf{x}}^{(k)} O) = \tan \angle(\tilde{\mathbf{y}}^{(k)} \tilde{\mathbf{x}}^{(k)} \tilde{\mathbf{x}}^{(k-1)}) = \frac{\|\tilde{\mathbf{y}}^{(k)} - \tilde{\mathbf{x}}^{(k-1)}\|}{(1-w)\|\tilde{\mathbf{y}}^{(k)}\|} = \frac{1}{(1-w) \tan \theta^{(k)}}, \quad (20)$$

and as a result $\theta^{(k)} = \theta^{(k+2)}$ for all $k \geq 1$. In addition, $\|\tilde{\mathbf{x}}^{(k)}\|/\|\tilde{\mathbf{x}}^{(k-1)}\| = w\|\tilde{\mathbf{y}}^{(k)}\|/\|\tilde{\mathbf{x}}^{(k-1)}\| = w \sin \theta^{(k)}$; therefore, it follows that

$$\frac{\|\tilde{\mathbf{x}}^{(k+1)}\|}{\|\tilde{\mathbf{x}}^{(k-1)}\|} = \frac{\|\tilde{\mathbf{x}}^{(k+1)}\|}{\|\tilde{\mathbf{x}}^{(k)}\|} \cdot \frac{\|\tilde{\mathbf{x}}^{(k)}\|}{\|\tilde{\mathbf{x}}^{(k-1)}\|} = w^2 \sin \theta^{(k+1)} \sin \theta^{(k)} = w^2 \sin \theta^{(1)} \sin \theta^{(2)}$$

making the left-hand side of (4) constant for all k , and equality will be obtained provided $\mathbf{x}^{(0)}$ and $\mathbf{x}^{(1)}$ are initialized such that $\sin \theta^{(1)} = 1/\sqrt{(2-w)}$. Then (20) implies that $\sin \theta^{(k)} = 1/\sqrt{(2-w)}$ for all $k \geq 1$. \square

Remark 5.1. *In addition, we can also specify the r -linear convergence factor. Since $\|\tilde{\mathbf{x}}^{(k)}\|/\|\tilde{\mathbf{x}}^{(k-1)}\| = w\|\tilde{\mathbf{y}}^{(k)}\|/\|\tilde{\mathbf{x}}^{(k-1)}\| = w \sin \theta^{(k)}$, it follows by similar arguments that the r -linear convergence factor is $w\sqrt{\sin \theta^{(1)} \sin \theta^{(2)}}$, which is bounded above by $w_0 = w/\sqrt{2-w}$ with the upper bound achieved when $\sin \theta^{(k)} = 1/\sqrt{(2-w)}$ for all $k \geq 1$, i.e., the setting described above such that (4) is an equality.*

5.3 Proof of Proposition 3

Proof. Following Theorem 1, we only need to consider the case $\lambda_{\max}(\mathbf{W}) = -\lambda_{\min}(\mathbf{W})$ and $m \geq 2$. We first claim that under this setting,

$$\|\tilde{\mathbf{x}}^{(k+2)}\| < \|\mathbf{W}\|^3 \|\tilde{\mathbf{x}}^{(k-1)}\| \quad (21)$$

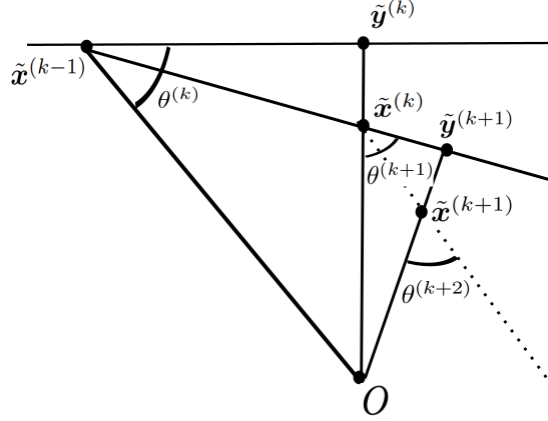


Figure 12: A visualization of AA(1) when \mathbf{W} is a scalar matrix.

for all $k \geq 1$. We prove (21) by contradiction. First, we note since $\|\tilde{\mathbf{x}}^{(k-1)}\| \geq \|\tilde{\mathbf{y}}^{(k)}\|$ and $\tilde{\mathbf{x}}^{(k)} = \mathbf{W}\tilde{\mathbf{y}}^{(k)}$,

$$\|\tilde{\mathbf{x}}^{(k)}\| = \|\mathbf{W}\tilde{\mathbf{y}}^{(k)}\| \leq \|\mathbf{W}\| \|\tilde{\mathbf{y}}^{(k)}\| \leq \|\mathbf{W}\| \|\tilde{\mathbf{x}}^{(k-1)}\| \quad (22)$$

with equality only achieved when $\tilde{\mathbf{y}}^{(k)} = \tilde{\mathbf{x}}^{(k-1)}$ and $\|\mathbf{W}\tilde{\mathbf{y}}^{(k)}\| = \|\mathbf{W}\| \|\tilde{\mathbf{y}}^{(k)}\|$. Assume

$$\|\tilde{\mathbf{x}}^{(k+2)}\| = \|\mathbf{W}\|^3 \|\tilde{\mathbf{x}}^{(k-1)}\|, \quad (23)$$

then following the analysis of (22) above, it holds only when for $i = 0, 1, 2$,

$$\tilde{\mathbf{y}}^{(k+i)} = \tilde{\mathbf{x}}^{(k-1+i)}, \quad \|\mathbf{W}\tilde{\mathbf{y}}^{(k+i)}\| = \|\mathbf{W}\| \|\tilde{\mathbf{y}}^{(k+i)}\|.$$

Since $\|\mathbf{W}\tilde{\mathbf{y}}^{(k)}\| = \|\mathbf{W}\| \|\tilde{\mathbf{y}}^{(k)}\|$, $\tilde{\mathbf{y}}^{(k)}$ lies in the span of the eigenvectors of \mathbf{W} with eigenvalues $\pm\|\mathbf{W}\|$. Let $\tilde{\mathbf{y}}^{(k)} = x_1\mathbf{v}_1 + x_2\mathbf{v}_2$, where \mathbf{v}_1 and \mathbf{v}_2 are eigenvectors of \mathbf{W} with eigenvalues $\|\mathbf{W}\|$ and $-\|\mathbf{W}\|$ respectively. Then $\tilde{\mathbf{x}}^{(k-1)} = \tilde{\mathbf{y}}^{(k)} = x_1\mathbf{v}_1 + x_2\mathbf{v}_2$, $\tilde{\mathbf{x}}^{(k)} = \mathbf{W}\tilde{\mathbf{y}}^{(k)} = \|\mathbf{W}\|(x_1\mathbf{v}_1 - x_2\mathbf{v}_2)$, and $\tilde{\mathbf{x}}^{(k+1)} = \|\mathbf{W}\|^2(x_1\mathbf{v}_1 + x_2\mathbf{v}_2)$. Let L_0 be the subspace containing $\tilde{\mathbf{x}}^{(k+1)}$, $\tilde{\mathbf{x}}^{(k)}$, $\tilde{\mathbf{x}}^{(k-1)}$, \dots , $\tilde{\mathbf{x}}^{(k-m_k+1)}$, then L_0 contains the line connecting $\tilde{\mathbf{x}}^{(k-1)}$ and $\tilde{\mathbf{x}}^{(k+1)} = \|\mathbf{W}\|^2\tilde{\mathbf{x}}^{(k-1)}$, so L_0 contains the origin. Recall that $\tilde{\mathbf{y}}^{(k+2)}$ is the point on L_0 with the smallest norm, so we must have $\tilde{\mathbf{y}}^{(k+2)} = \mathbf{0}$, which means that $\tilde{\mathbf{x}}^{(k+2)} = \mathbf{W}\tilde{\mathbf{y}}^{(k+2)} = \mathbf{0}$, violating our assumption in (23), and as a result (21) must hold.

Next, we prove

$$\|\tilde{\mathbf{x}}^{(k+2)}\| \leq c\|\mathbf{W}\|^3\|\tilde{\mathbf{x}}^{(k-1)}\| \quad (24)$$

for some $c < 1$ by a similar contradiction argument. If (24) does not hold, then (22) implies that for $i = 0, 1, 2$,

$$\|\tilde{\mathbf{y}}^{(k+i)}\| > c\|\tilde{\mathbf{x}}^{(k-1+i)}\|, \quad \|\mathbf{W}\tilde{\mathbf{y}}^{(k+i)}\| > c\|\mathbf{W}\| \|\tilde{\mathbf{y}}^{(k+i)}\|. \quad (25)$$

Recall that $\tilde{\mathbf{x}}^{(k-1+i)} - \tilde{\mathbf{y}}^{(k+i)} \perp \tilde{\mathbf{y}}^{(k+i)}$, the first inequality in (25) implies that $\tilde{\mathbf{x}}^{(k-1+i)}$ is close to $\tilde{\mathbf{y}}^{(k+i)}$ in the sense that

$$\frac{\|\tilde{\mathbf{x}}^{(k-1+i)} - \tilde{\mathbf{y}}^{(k+i)}\|}{\|\tilde{\mathbf{y}}^{(k+i)}\|} < \frac{\sqrt{1-c^2}}{c},$$

and note that its RHS approaches zero as $c \rightarrow 1$.

The second inequality in (25) implies that when c is close to 1, $\tilde{\mathbf{y}}^{(k+i)}$ approximately lies in the span of the eigenvectors of \mathbf{W} with eigenvalues $\pm\|\mathbf{W}\|$. In particular, let L_1 and L_2 be the eigenspaces of \mathbf{W} with eigenvalues $\pm\|\mathbf{W}\|$, $\{\lambda_i(\mathbf{W})\}_{i=1}^n$ be the eigenvalues of \mathbf{W} , and $\beta = \max_{i:\lambda_i(\mathbf{W}) \neq \pm\|\mathbf{W}\|} |\lambda_i(\mathbf{W})|/\|\mathbf{W}\|$, then $0 \leq \beta < 1$ and the second inequality in (25) implies

$$\|P_{L_1 \oplus L_2} \tilde{\mathbf{y}}^{(k+i)}\|^2 + \beta^2 \|\tilde{\mathbf{y}}^{(k+i)} - P_{L_1 \oplus L_2} \tilde{\mathbf{y}}^{(k+i)}\|^2 > c^2 \|\tilde{\mathbf{y}}^{(k+i)}\|^2,$$

so

$$\|\tilde{\mathbf{y}}^{(k+i)} - P_{L_1 \oplus L_2} \tilde{\mathbf{y}}^{(k+i)}\|^2 < \frac{1-c^2}{1-\beta^2} \|\tilde{\mathbf{y}}^{(k+i)}\|^2,$$

meaning that $\tilde{\mathbf{y}}^{(k+i)}$ approximately lies in the span of the eigenvectors of \mathbf{W} with eigenvalues $\pm\|\mathbf{W}\|$. Again, the RHS goes to zero as c approaches 1.

Following a similar argument to the proof of (21), we are able to show that when c is sufficiently close to 1, $\|\tilde{\mathbf{x}}^{(k+1)} - \|\mathbf{W}\|^2 \tilde{\mathbf{x}}^{(k-1)}\|/\|\tilde{\mathbf{x}}^{(k+1)}\| \approx 0$, which means $\|\tilde{\mathbf{y}}^{(k+2)}\|/\|\tilde{\mathbf{x}}^{(k+1)}\| \approx 0$, and it is a contradiction to the assumption that (24) does not hold, which in turn proves (24).

We prove the second half of the proposition with an example. Let $|w| < 1$, $\mathbf{W} := \text{Diag}(w, -w)$, $\mathbf{a} := \mathbf{0}$, $\tilde{\mathbf{x}}^{(0)} = [u, v]$ such that $(1-w)u^2 = (1+w)v^2$. Then AA(1) applied to this problem generates the sequences $\tilde{\mathbf{y}}^{(k)} = \tilde{\mathbf{x}}^{(k-1)}$ and $\tilde{\mathbf{x}}^{(k)} = \mathbf{W} \tilde{\mathbf{y}}^{(k)}$ for all $k \geq 2$. Therefore, AA(1) is reduced to the fixed-point method and it converges r -linearly with rate $\|\mathbf{W}\|$. \square

5.4 Proof of Theorem 4

Proof. The proof is similar to that of the proof of Theorem 1. Assuming that $\mathbf{x}_* = \mathbf{0}$, let $\tilde{\mathbf{x}}^{(k)} = q(\mathbf{x}^{(k)} - \mathbf{x}^{(k)})$ and

$$\tilde{\mathbf{y}}^{(k+1)} = \sum_{j=k-m_k}^k \alpha_j^{(k)} \tilde{\mathbf{x}}^{(j)} = \sum_{j=k-m_k}^k \alpha_j^{(k)} (q(\mathbf{x}^{(j)}) - \mathbf{x}^{(j)}),$$

and

$$\tilde{\mathbf{x}}^{(k+1)} = (q - \mathbf{I})\mathbf{x}^{(k+1)} = (q - \mathbf{I}) \left(\sum_{j=k-m_k}^k \alpha_j^{(k)} q(q - \mathbf{I})^{-1}(\tilde{\mathbf{x}}^{(j)}) \right). \quad (26)$$

Next, we claim the following three properties hold:

1. $\|\tilde{\mathbf{y}}^{(k+1)}\| \leq \|\tilde{\mathbf{x}}^{(k)}\|$, with $\angle(\mathbf{O}\tilde{\mathbf{y}}^{(k+1)}\tilde{\mathbf{x}}^{(k)}) \geq \pi/2$.
2. $\tilde{\mathbf{x}}^{(k+1)} = q(\tilde{\mathbf{y}}^{(k+1)}) + (\max_{k-m_k \leq j \leq k} \|\mathbf{x}^{(j)}\|^2)C_1^2$.
3. $q(\mathbf{x}) \leq (\|\mathbf{W}\| + C_2\|\mathbf{x}\|)\|\mathbf{x}\|$.

The first property follows from the definition of $\tilde{\mathbf{y}}^{(k+1)}$ in (7). Note that we have $\angle(\mathbf{O}\tilde{\mathbf{y}}^{(k+1)}\tilde{\mathbf{x}}^{(k)}) \geq \pi/2$ instead of $\angle(\mathbf{O}\tilde{\mathbf{y}}^{(k+1)}\tilde{\mathbf{x}}^{(k)}) = \pi/2$ as in the proof of Theorem 1, due to the constraint that $\alpha_j^{(k)}$ are bounded. The second property is proved using (26). Note that locally, $q(\mathbf{x})$ is approximated with its first-order expansion at \mathbf{x}_* with an error in the order of $\|\mathbf{x} - \mathbf{x}_*\|^2$, and $\alpha_j^{(k)}$ are bounded, the second point is proved. The third property follows from approximation of q with its first-order expansion at $\mathbf{x}_* = 0$.

We first prove that AA(m) converges when the initialization is sufficiently close to \mathbf{x}_* . Let a sequence $d^{(k)}$ generated by $d^{(1)} = \|\tilde{\mathbf{x}}^{(1)}\|$ and $d^{(k+1)} = (\|\mathbf{W}\| + C_2d^{(k)})d^{(k)} + (\max_{k-m_k \leq j \leq k} d^{(j)2})C_1^2$, the the properties above implies that $\|\tilde{\mathbf{x}}^{(k)}\| \leq d^{(k)}$; and it is clear from definition that $d^{(k)}$ converges to zero when $d^{(1)}$ is small.

Next, we will prove the r -linear convergence factor of $\tilde{\mathbf{x}}^{(k)}$ is at least $\sqrt{w_0\|\mathbf{W}\|}$. To prove it, it is sufficient to prove that for there exists a sufficiently large K_0 such that for any large $k > K_0$, there exists some $k_0 < k$ such that

$$\frac{\|\tilde{\mathbf{x}}^{(k)}\|}{\|\tilde{\mathbf{x}}^{(k_0)}\|} \leq (w_0\|\mathbf{W}\|)^{(k+1-k_0)/2}. \quad (27)$$

When $\max_{k-m_k \leq j \leq k} \|\mathbf{x}^{(j)}\| \leq (w_0\|\mathbf{W}\|)^{-m_k/2}\|\tilde{\mathbf{x}}^{(k+1)}\|$, this equality holds naturally by applying the property 3. Otherwise, $\max_{k-m_k \leq j \leq k} \|\mathbf{x}^{(j)}\|^2$ is bounded above. Similar to the proof in Theorem 1 and note that the second-order terms in Taylor expansion are sufficiently small, we have

$$\frac{\|\tilde{\mathbf{x}}^{(k+1)}\|}{\|\tilde{\mathbf{x}}^{(k-1)}\|} \leq w_0\|\mathbf{W}\|, \quad (28)$$

which implies (27). We remark that while there is an additional upper bound of coefficient $\alpha_j^{(k)}$, it does not change the analysis: When the upper bound C_0 is larger than some constant depending \mathbf{M} , $\hat{\mathbf{y}}^{(k+1)}$ in Figure 10 is a linear combination of $\tilde{\mathbf{x}}^{(k+1)}$ and $\tilde{\mathbf{x}}^{(k)}$ with coefficients not larger than C_0 and can be achieved in optimization (7), and the fact that $\angle(\mathbf{O}\tilde{\mathbf{y}}^{(k+1)}\tilde{\mathbf{x}}^{(k)}) \geq \pi/2$ (instead of being equal) does not change the upper bound of $\angle(\mathbf{O}\tilde{\mathbf{x}}^{(k-1)}\tilde{\mathbf{x}}^{(k)})$. As a result, (27) is proved for sufficiently large $k > K_0$, and the r -linear convergence factor of AA(m) is proved. \square

6 Conclusion

This paper studies the convergence properties of Anderson acceleration and provides the first argument showing it improves the root-linear convergence factor of the fixed-point iteration when q is

linear and symmetric. We extend our investigation to nonlinear operators q possessing a symmetric Jacobian at the solution and prove an adapted version of AA locally enjoys improved root-linear convergence. Our theoretical discoveries were validated through simulations where we showcased Anderson acceleration significantly outperforms the fixed-point iteration for Tyler’s M-estimation. In the future, we hope to generalize our results to non-symmetric linear operators and refine the estimations of the r -linear convergence factor.

Acknowledgements

First, GL thanks Yousef Saad for introducing him to Anderson Acceleration. The authors also thank and acknowledge their funding sources as this material is based upon work supported by the National Science Foundation Graduate Research Fellowship Program under Grant No. 2237827, NSF Award DMS-2124913, and NSF DMS-2318926. Any opinions, findings, and conclusions or recommendations expressed in this material are those of the author(s) and do not necessarily reflect the views of the National Science Foundation.

References

- Anderson, D. G. (1965). Iterative procedures for nonlinear integral equations. *J. ACM*, 12(4):547–560.
- De Sterck, H. and He, Y. (2022). Linear asymptotic convergence of Anderson acceleration: Fixed-point analysis. *SIAM Journal on Matrix Analysis and Applications*, 43(4):1755–1783.
- Evans, C., Pollock, S., Rebholz, L. G., and Xiao, M. (2020). A proof that Anderson acceleration improves the convergence rate in linearly converging fixed-point methods (but not in those converging quadratically). *SIAM Journal on Numerical Analysis*, 58(1):788–810.
- Fang, H.-r. and Saad, Y. (2009). Two classes of multisection methods for nonlinear acceleration. *Numerical linear algebra with applications*, 16(3):197–221.
- Geist, M. and Scherrer, B. (2018). Anderson acceleration for reinforcement learning. *arXiv preprint arXiv:1809.09501*.
- Goes, J., Lerman, G., and Nadler, B. (2020). Robust sparse covariance estimation by thresholding tyler’s m-estimator.
- Kelley, C. T. (2018). Numerical methods for nonlinear equations. *Acta Numerica*, 27:207–287.
- Picard, É. (1890). Memoire sur la theorie des equations aux derivees partielles et la methode des approximations successives. *Journal de Mathématiques pures et appliquées*, 6:145–210.

- Pollock, S. and Rebholz, L. G. (2021). Anderson acceleration for contractive and noncontractive operators. *IMA Journal of Numerical Analysis*, 41(4):2841–2872.
- Pollock, S., Rebholz, L. G., and Xiao, M. (2019). Anderson-accelerated convergence of picard iterations for incompressible navier–stokes equations. *SIAM Journal on Numerical Analysis*, 57(2):615–637.
- Potra, F. A. and Engler, H. (2013). A characterization of the behavior of the Anderson acceleration on linear problems. *linear Algebra and its Applications*, 438(3):1002–1011.
- Pulay, P. (1980). Convergence acceleration of iterative sequences. the case of scf iteration. *Chemical Physics Letters*, 73(2):393–398.
- Rebholz, L. G. and Xiao, M. (2023). The effect of Anderson acceleration on superlinear and sublinear convergence. *Journal of Scientific Computing*, 96(2):34.
- Scieur, D. (2019). Generalized framework for nonlinear acceleration.
- Scieur, D., d'Aspremont, A., and Bach, F. (2016). Regularized nonlinear acceleration. *Advances in Neural Information Processing Systems*, volume 29. Curran Associates, Inc.
- Shi, W., Song, S., Wu, H., Hsu, Y.-C., Wu, C., and Huang, G. (2019). Regularized Anderson acceleration for off-policy deep reinforcement learning. *Advances in Neural Information Processing Systems*, 32.
- Sun, K., Wang, Y., Liu, Y., Pan, B., Jui, S., Jiang, B., Kong, L., et al. (2021). Damped Anderson mixing for deep reinforcement learning: Acceleration, convergence, and stabilization. *Advances in Neural Information Processing Systems*, 34:3732–3743.
- Toth, A. and Kelley, C. T. (2015). Convergence analysis for Anderson acceleration. *SIAM Journal on Numerical Analysis*, 53(2):805–819.
- Tyler, D. E. (1987a). A distribution-free m-estimator of multivariate scatter. *The Annals of Statistics*, 15(1):pp. 234–251.
- Tyler, D. E. (1987b). Statistical analysis for the angular central Gaussian distribution on the sphere. *Biometrika*, 74: pp. 579–589.
- Frahm, G. and Jaekel, U. (2010) A generalization of Tyler’s M-estimators to the case of incomplete data. *Comput. Statist. Data Anal.*, 54: pp. 374–393.
- Chen, Y., Wiesel, A., and Hero, A. O. (2011) Robust shrinkage estimation of high-dimensional covariance matrices. *IEEE Trans. Signal Process.*, 59: pp. 4097–4107.

- Ollila, E. and Koivunen, V. (2003) Robust antenna array processing using M-estimators of pseudo-covariance *IEEE 14th International Symposium on Personal, Indoor and Mobile Radio Communications (PIMRC)*, pp. 2659–2663.
- Ollila, E. and Tyler, D. E. (2012) Distribution-free detection under complex elliptically symmetric clutter distribution *IEEE 7th Sensor Array and Multichannel Signal Processing Workshop, (SAM)* , pp. 413–416.
- Kent, J. T. and Tyler, D. E. (1988). Maximum likelihood estimation for the wrapped Cauchy distribution. *Journal of Applied Statistics*, 15(2):pp. 247–254.
- Franks, W. C. and Moitra, A. (2020). Rigorous Guarantees for Tyler’s M-Estimator via Quantum Expansion. *Conference on Learning Theory*, PMLR 125: pp. 1601-1632.
- Frahm, G. and Jaekel, U. (2007). Tyler’s M-estimator, random matrix theory, and generalized elliptical distributions with applications to finance. Discussion Papers in Econometrics and Statistics, No. 2/07, University of Cologne, Institute of Econometrics and Statistics.
- Walker, H. F. and Ni, P. (2011). Anderson acceleration for fixed-point iterations. *SIAM Journal on Numerical Analysis*, 49(4):1715–1735.
- Zhang, T., Cheng, X., and Singer, A. (2016). Marčenko-pastur law for tyler’s m-estimator. *J. Multivar. Anal.*, 149:114–123.